# Local Rotation Pattern: A Local Descriptor of Color Textures

Hela Jebali[1], Noël Richard[2] and Mohamed Naouai[1]
[1]*Faculty of Science of Tunis, University Campus El Manar, Tunisia*
[2]*University of Poitiers, XLIM UMR CNRS 6172, France*

Keywords: Color Texture, Descriptor, Quaternion Rotation, Geodesic Distance, Classification.

Abstract: Describing color textures is an extremely challenging problem in pattern recognition and computer vision. In this paper, a new texture feature is proposed and investigated for color texture image classification. Based on quaternion representation of color images and quaternion rotation, a Local Rotation Pattern descriptor (LRP) is proposed. Using quaternion to represent color images is done by encoding the three RGB channels into the three imaginary parts of a quaternion. The distance between two color can be expressed as the angle of rotation between two unit quaternions using the geodesic distance to obtain finally our LRP histograms. Performance in texture classification is assessed for three challenging datasets: Vistex, Outex-TC13 and USPtex databases facing to the recent results from the state-of-the-art. Results show the high efficiency of the proposed approach.

## 1 INTRODUCTION

Colour is an important characteristic of digital images which has received significant interest from the research community. This fundamental image property has been widely used in many applications such as object recognition, skin detection and image retrieval. Although, a large variety of efficient texture descriptors has been developed in the literature.

Cooccurrence matrix and Run-Length Matrix (RLM)(Xiaoyan et al., 2009) are good descriptors of texture content. Some years later, Ojala (Ojala et al., 2002) expanded the local binary pattern (LBP) as a powerful and successful texture descriptor in pattern recognition and many computer vision applications. The Local Binary Pattern descriptor has been used successfully in texture classification (Guo et al., 2012) , face recognition (Timo et al., 2004) and image retrieval (Penatti et al., 2012). Several research works have proposed to transpose the texture analysis from gray-level to colour images (Guo et al., 2010)(Guo et al., 2010)(Mehta and Egiazarian, 2016). Several colour texture expression are induced by the analysis of color as a combination of three gray-level texture affected to the three colour channel. It exists few works express the vectorial processing of color texture.

For research in computer graphics and computer vision, Rotations in three-dimensional space are commonly represented as unit quaternions in a relatively simple way. In this work, based on a local pattern encoding scheme and the quaternion representation, we propose to use the rotation notion to process the distance between colors. Therefore, a new vector texture feature: Local Rotation Pattern (LRP) is suggested. This paper is organised as follow: in the following sections, the mathematical definition of quaternion and its properties are recalled. Then, we detailed the Local Rotation Pattern (LRP) proposition and the associated feature. Finally, the performance of our proposed descriptor is evaluated on three challenging datasets: Vistex, Outex-TC13 and USPtex databases.

## 2 QUATERNION ALGEBRA

### 2.1 Definition

Quaternions were discovered by William Hamilton in 1843 (Rowan, 1866) with the aim of generalize complex numbers in three dimensional space. Quaternions form a four dimensional noncommutative algebra. Extended from the complex numbers, any quaternion $q \in \mathbb{H}$ can be written in its Cartesian form as:

$$q = w + xi + yj + zk \quad (1)$$

where $w,x,y,k \in \mathbb{R}$ and $i,j,k$ are complex operators that are roots of $-1$ satisfying:

$$i^2 = j^2 = k^2 = ijk = -1 \quad (2)$$

$$(ij = -ji = k),(jk = -kj = i),(ki = -ik = j) \quad (3)$$

The real number a is called a real (or scalar) part of $q$ and is denoted $\mathcal{R}(q)$. The quaternion with real



Jebali, H., Richard, N. and Naouai, M.
Local Rotation Pattern: A Local Descriptor of Color Textures.
DOI: 10.5220/0009827805670573
In *Proceedings of the 15th International Conference on Software Technologies (ICSOFT 2020)*, pages 567-573
ISBN: 978-989-758-443-5

part $w = 0$, called pure quaternion ($q = xi + yj + zk$), is an imaginary (or vector) part of $q$ and is denoted $I(q)$. We can thus write $q = \mathcal{R}(q) + I(q)$.
The quaternion conjugate is $\overline{q} = \mathcal{R}(q) - I(q)$ and the modulus of a quaternion is given by:

$$|q| = \sqrt{w^2 + x^2 + y^2 + z^2} = \sqrt{q\overline{q}} \quad (4)$$

Any quaternion with a norm $|q| = 1$ is named a unit quaternion. The inverse of any quaternion is defined as $q^{-1} = \frac{\overline{q}}{|q|}$, such that $qq^{-1} = 1$. Hence, any quaternion may be represented in the polar form:

$$q = |q| \exp^{\mu\theta} = |q|(\cos\theta + \mu \sin\theta) \quad (5)$$

Where $\mu = \frac{xi+yj+zk}{\sqrt{xi+yj+zk}}$ and $\theta = \arccos(\frac{w}{|q|})$ represent a real angle.

## 2.2 Quaternion RGB Images

Sangwine (Sangwine, 1996) was the first to demonstrate the applicability of a quaternion Fourier transform to color images. A color containing only three components in the RGB space, Sangwine proposed to describe the color information on the imaginary part of the pure quaternion. Any pixel of a image $I$ at the coordinates (x,y) will therefore be coded as follows:

$$I(x,y) = 0 + R(x,y)i + Gx,y)j + B(x,y)k \quad (6)$$

Where $R(x,y), G(x,y)$ and $B(x,y)$ represent the components Red, green and blue respectively. Figure 1 illustrates the quaternion representation of RGB color images.

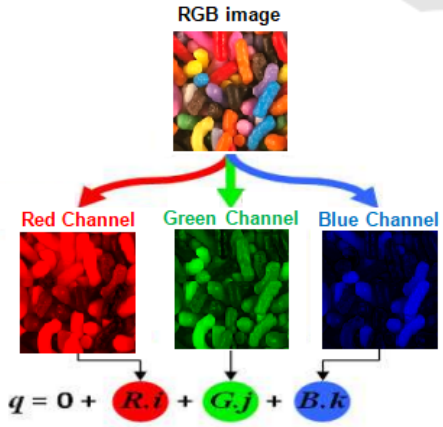


Figure 1: Quaternion Representation of RGB color image.

Quaternions are compactly represent the RGB color space. Therefore, the color interaction that exists between different channels is incorporated in any processing at the image level.

## 2.3 Distance between Quaternions as Rotations

Rotation in three-dimensional space can be represented in various forms. The Euler angles and quaternions are the two commonly used forms in computer vision applications. In this work, we interested to the quaternion representation. Any rotation $R$ can be described using a unit quaternion $r$ (with norm equal to 1) as follows:

$$r = \cos(\frac{\theta}{2}) + v\sin(\frac{\theta}{2}) \quad (7)$$

Where $\theta$ and $v$ are respectively the angle and axis of the rotation $R$.

In the unit-quaternion system, the concept of the distance between two rotations can be described by the angle between them. In geometry, this distance is the length of the shortest geodesic path on the manifold $\mathbb{H}$ between both quaternions. This distance is called the Riemannian distance between two quaternions $q_1$ and $q_2$ is given by:

$$dist_{\mathbb{H}}(q_1, q_2) = \|\log(q_1^{-1} q_2)\| \quad (8)$$

Where $\log(q_i)$ gives the rotation axis and angle of the rotation matrix. The $\|.\|$ above gives the magnitude of the rotation angle. This Riemannian metric is well known in the case of unit quaternions. The property of the invariance to inversion of $q_1^{-1}q_2 \neq q_2 q_1^{-1}$ gives:

$$\|\log(q_1^{-1} q_2)\| = \|\log(q_1 q_2^{-1})\| \quad (9)$$

Angulo in (Jesús, 2014) proposed a symmetrized version of the geodesic distance between two unit quaternions as follows:

$$dist_{\mathbb{H}}(q_1, q_2) = \|\log(q_1^{-\frac{1}{2}} q_2 q_1^{-\frac{1}{2}})\| \quad (10)$$

Where the norm represent the usual Euclidean norm. This geodesic distance gives values in the range $[0, \pi]$.

# 3 PROPOSED METHOD

## 3.1 Local Rotation Pattern (LRP)

In this section, we describe the proposed vector feature for color texture: Local Rotation Pattern *LRP*. Our proposed pattern intends to explore the difference between two adjacent color pixels based on quaternion representation. Suppose $q_i$ and $q_j$ are two quaternions in color image, Figure 2 shows that the two quaternions differ in their amplitudes as well as in the phase $\theta$ that exists between them. Therefore, there are two options to process the difference or the similarity

between two color pixels: the first one is the modulus as following:

$$h(q_i, q_j) = |q_i| - |q_j| \quad (11)$$

Furthermore the modulus, the phase between the two quaternions can also be used to express the difference between them using the Eq. 10. In the case of two similar quaternions, we found that the modulus difference and the phase θ are equal to zero.

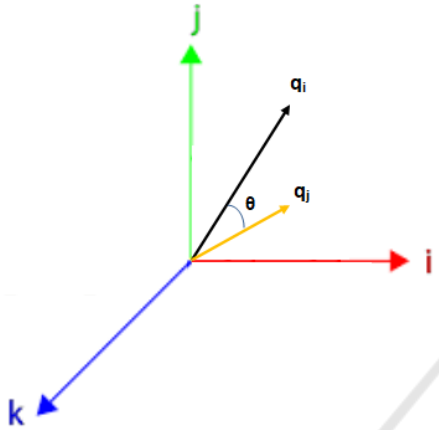


Figure 2: Illustration of the difference between two quaternion $q_i$ and $q_j$.

Following, based on quaternion representation of color image, two local pattern are used to coded our proposed Local Rotation Pattern *LRP*: one for the norms $LRP_N$ and the other for the angle of rotation $LRP_A$. Given a color image $I$ represented in a quaternion form. Based on the local pattern scheme, let $q_c$ the quaternion central pixel of $3 \times 3$ block with $P = 8$ neighbors and $q_i$ are the surrounding pixels. The local pattern of norms $LRP_N$ of the central pixel is replaced by the mean of the various norm difference calculated using Eq. 11.

More details of our local pattern value for $LRP_N$ are given in Figure 3 using the Eqs. 12 and 13.

$$LRP_N(q_c) = \frac{1}{P}\sum_{i=0}^{P-1} h(q_i, q_c) \quad (12)$$

$$Hist(LRP_N) = \{prob(LRP_N = a), \forall a \in [0, 255]\} \quad (13)$$

In other hand, considering color as a unit quaternion, it can represent a rotation in three dimensional. Therefore, the distance between central pixel and its surrounding are expressed as a distance between two rotations using the geodesic distance using Eq. 10. Finally, the Local Pattern value of $LRP_A$ of the central pixel $q_c$ is then coded with the average value of the different angles rotation, as given by:

$$LRP_A(q_c) = \frac{1}{P}\sum_{i=0}^{P-1} dist_{\mathbb{H}}(q_i, q_c) \quad (14)$$

$$Hist(LRP_A) = \{prob(LRP_A = a), \forall a \in [0, \pi]\} \quad (15)$$

Eventually, the *LRP* signature of texture I is defined by concatenate the two histograms of two local patterns $LRP_A$ and $LRP_N$ as:

$$Hist(LRP) = \{Hist(LRP_A), Hist(LRP_N)\} \quad (16)$$

The process of encoding LRP is illustrated in Figure 3.

### 3.2 Similarity Measure between LRP

Similarity measure plays an important role to retrieve textures. Many distance functions can be used to measure similarities, between features. Considering the LRP as probability density function, the mostly used similarity measure is the Kullback-Leibler divergence. The Kullback-Leibler measure of information $KL(P/Q)$ assess the quantity of information lost when $Q$ is used to estimate $P$ (Eq. 17) (Kullback and Leibler, 1951).

$$KL(P/Q) = \int_{-\infty}^{\infty} p(x) \ln\left(\frac{p(x)}{q(x)}\right) dx \quad (17)$$

where p and q are the respective densities of $P$ and $Q$. In order to define a similarity measure, the Kullback-Leibler divergence is defined as the sum of the measure of information of $P$ relative to $Q$ and the measure of information of $Q$ relative to $P$.

$$D_{KL}(P, Q) = KL(P/Q) + KL(Q/P) \quad (18)$$

## 4 EXPERIMENTS AND DISCUSSION

This section provides several experimental results to demonstrate the effectiveness of the proposed LRP. We evaluate the proposed color feature using a challenging problems: color image classification. In order to assess classification performances of the suggested LRP feature, we used the standard protocol used in (Maliani et al., 2014). Images of each databases are divided into two sub-sets, where 50% are used for training phase and the other 50% for validation. Each image of the test set is the classified through the nearest neighbor class (1-NN) with the less Kullback-Leibler divergence ($D_{KL}$ distance).

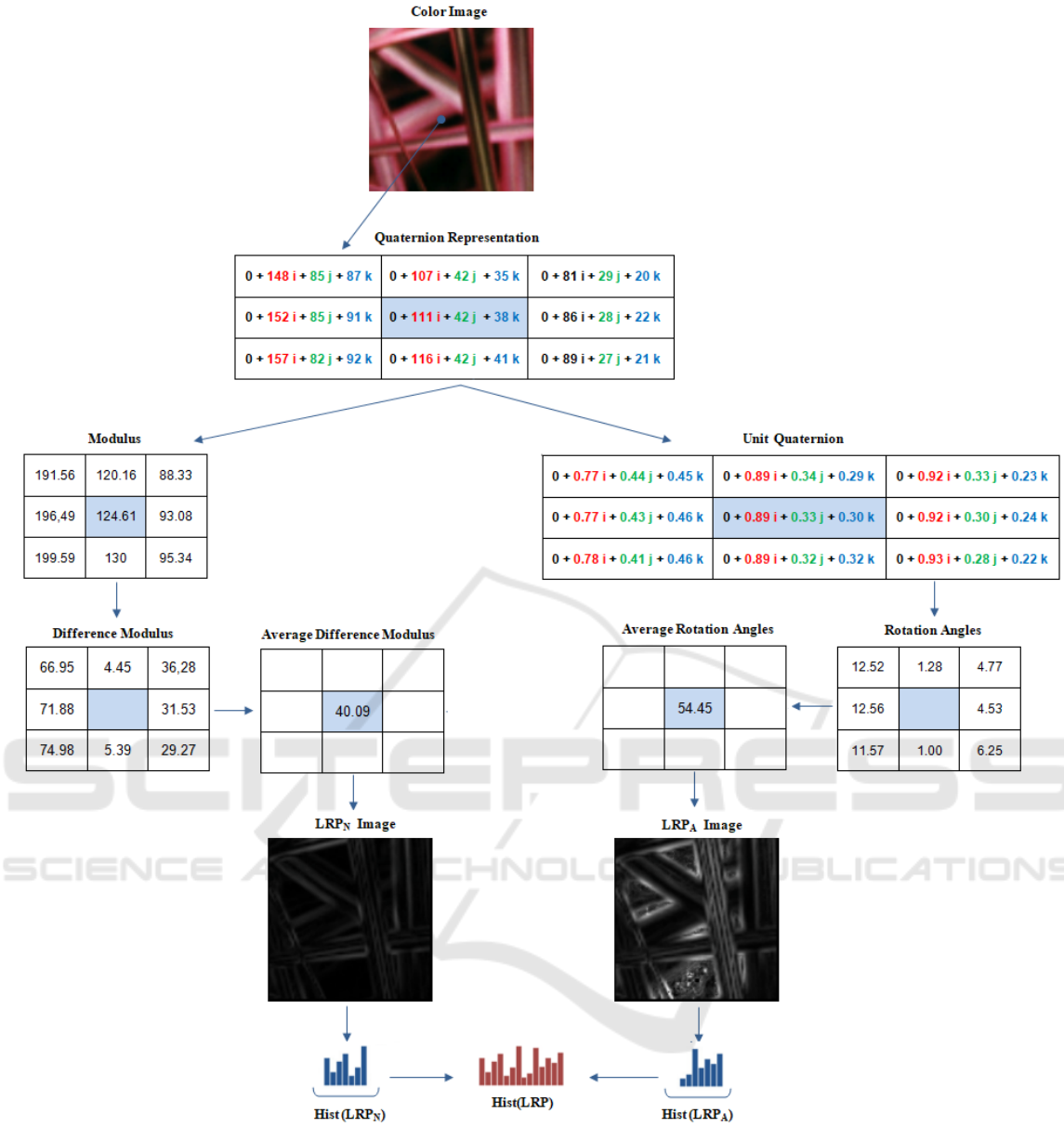


Figure 3: The basic LRP descriptor with $P = 8$.

## 4.1 Dataset and Results

For experimentation and in order to show the high efficiency of the proposed descriptor, three following popular color texture databases from the literature are used: *Vistex*[1], *Outex-TC13*[2], and *USPtex*[3] databases:

Vistex is one of the most used dataset for comparative study. It is built of 54 colour images of size $512 \times 512$ pixels, these images are acquired using uncontrolled conditions. Each colour image was divided into 16 sub-images of $128 \times 128$ pixels, resulting 432 images. The Figure 4 presents some classes of *Vistex* dataset with their two local patterns $LRP_N$ and $LRP_A$, which the inter and intra-class $D_{KL}$ distance between them are shows in Table 1.

The distance between classes varies according to the similarity between them while the inter-class distance is equal zero. Following distances, there are resemblance between *Fabric* and the *Food* (251.72).

*USPtex* dataset (Andre et al., 2012) contains 191

[1]http://vismod.media.mit.edu/vismod/imagery/VisionTexture

[2]http://www.outex.oulu.fi

[3]http://fractal.ifsc.usp.br/dataset/USPtex.php

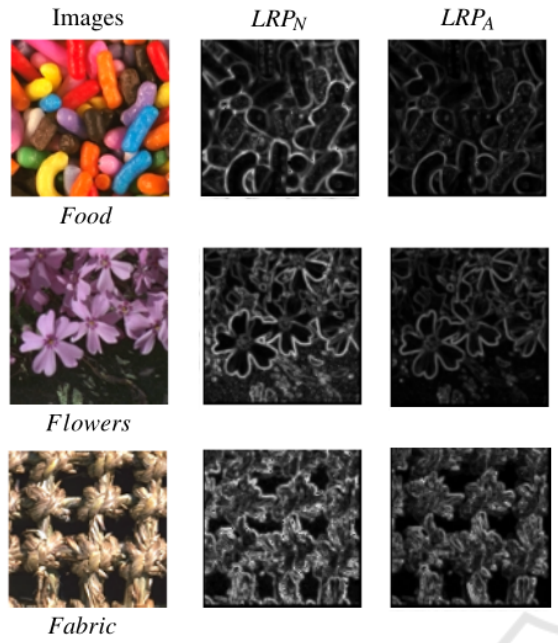


Figure 4: Some color textures from Vistex dataset with their $LRP_A$ and $LRP_N$.

classes of natural colored textures, found on a daily basis. The original images of size $512 \times 384$ are divided into 12 samples of size $128 \times 128$, so 2292 images in total. Figure 5 shows three different color textures from this database (*Brick*, *Leaves* and *Grass* textures) and the Table 2 presents the similarity measure between them.

Table 1: Inter and intra-class $D_{KL}$ distance for images of Vistex database.

| *Vistex* | *Fabric* | *Flowers* | *Food* |
|---|---|---|---|
| *Fabric* | 0 | 593.65 | 949.83 |
| *Flowers* | 593.65 | 0 | 251.72 |
| *Food* | 949.83 | 251.72 | 0 |

Table 2: Inter and intra-class $D_{KL}$ distance for color images of Outex-TC13 database.

| *USPtex* | *Brick* | *Leaves* | *Grass* |
|---|---|---|---|
| *Brick* | 0 | 3171.95 | 3826.54 |
| *Leaves* | 3171.95 | 0 | 1396.28 |
| *Grass* | 3826.54 | 1396.28 | 0 |

The *Outex* database contains 1360 images divided into 68 classes with 20 samples per class of size $128 \times 128$ pixels. Figure 6 shows some color textures of *Outex* database with their two local patterns $LRP_N$ and $LRP_A$.

Visually, we can observe the great similarity between the two *Barleyrice* classes. This similarity is validated by the estimated Kullback-Leibler Divergence $D_{KL} = 632.75$ (see Table 4). On the other hand the *Barley 09* texture is far from the *Canvas* texture visually, that is expressed by the distance value $D_{KL} = 3448.59$.


Figure 5: Some color textures from USPtex dataset with their $LRP_A$ and $LRP_N$.

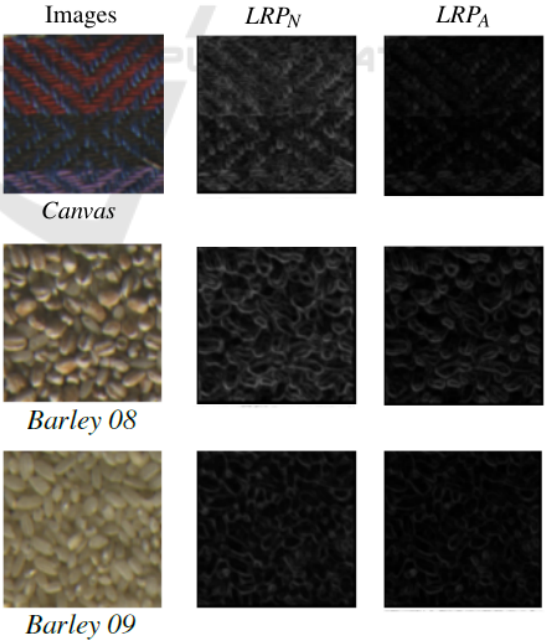


Figure 6: Some color textures from Outex-TC13 dataset with their $LRP_A$ and $LRP_N$.

Table 3: Classification rates (%) achieved by the proposed LRP on Vistex, Outex-TC13 and USPtex databases in front of results previously published. Best results reached are highlighted by bold text.

| Methods | Vistex | Outex-TC13 | USPtex |
|---|---|---|---|
| LSTM network (Byeon et al., 2014) | 99.09 | 94.70 | - |
| SMGD (Maliani et al., 2014) | 97.50 | 89.70 | - |
| Local jet+ Fourier (Oliveira et al., 2015) | 97.84 | 87.16 | 89.63 |
| $C_2O$ (Martinez et al., 2015) | 99.30 | 82.64 | - |
| CLP (Richard et al., 2016) | 97.70 | 82.10 | - |
| LED+ED (Minh-Tan et al., 2017) | 94.70 | 76.67 | 90.50 |
| LNDP (Manisha and Balasubramanian, 2017) | - | 77.16 | 80.66 |
| SMO (Neiva et al., 2018) | 99.54 | 86.47 | 91.49 |
| LDTP (Khadiri et al., 2018) | 75.82 | 80.32 | 84.11 |
| Relocated $C_2O$ (Jebali et al., 2018) | **100** | 92.40 | - |
| LCCMSP (Merabet and Ruichek, 2018) | - | 84.87 | 90.01 |
| ARCS-LBP (Merabet et al., 2019) | - | 85.72 | 88.88 |
| Proposed LRP | 99.54 | **94.90** | **93.20** |

Table 4: Inter and intra-class $D_{KL}$ distance for color images of Outex-TC13 database.

| *Outex* | *Canvas* | *Barley 08* | *Barley 09* |
|---|---|---|---|
| *Canvas* | 0 | 1781.34 | 3448.59 |
| *Barley 08* | 1781.34 | 0 | 632.75 |
| *Barley 09* | 3448.59 | 632.75 | 0 |

### 4.2 Performance in Classification

To have a fair comparison of our obtained classification rates in front of those previously published, we used the same databases and the same schemes of partitions used for training and testing as in the recent published methods (Maliani et al., 2014), (Richard et al., 2016), (Jebali et al., 2018), (Neiva et al., 2018) and (Merabet et al., 2019).

A comparative analysis of obtained classification rates by the proposed texture descriptor and some state-of-the-art texture descriptors summarized in Table 3. The highest result of each dataset is highlighted in bold type. Firstly, for the *Vistex* database, the best classification rate is achieved by two methods: the Relocated $C_2O$ with 100% and the second row is achieved by the proposed LRP with 99.54%.

For *USPtex* dataset, the lowest results are obtained by the integrative methods LNDP, LDTP and ARCS-LBP (around 80.66%, 84.11% and 88.88%). The highest result is obtained using the proposed method achieving 93.20% of accuracy rate.

In terms of color texture characterization, *Outex-TC13* is the hardest database as results shows. Moreover, on this dataset the performance of LSTM network method around 94.70%. The Local directional ternary pattern (LDTP) and the Colour local pattern (CLP) descriptor presents the lowest accuracies, with 80.32% and 82.10% respectively. The highest performance is obtained by the proposed Local Rotation Pattern (LRP) with 94.90%.

## 5 CONCLUSION

In this paper, we proposed a new vector texture feature using the quaternion rotation. Unlike the existing texture feature, the proposed one enables the implicit use of the color interaction between color components in color images. The experiment results show the efficiently of our proposed texture descriptor for color texture image classification. Our proposed method was tested on three databases, the VisTex, Outex, and USPtex databases, yielding correct classification rates of 99.54%, 94.90% and 93.20% respectively. Future works will be devoted to improving the robustness of our proposed descriptor to color image changes (Rotation, scaling change, illuminance change).

## REFERENCES

Andre, B., Dalcimar, C., and Odemir, B. (2012). Color texture analysis based on fractal descriptors. *Pattern Recognition*, 45:1984–1992.

Byeon, W., Liwicki, M., and Breuel, T. (2014). Texture classification using 2d lstm networks. *IEEE, 22nd Int. C. Pattern Recogn. (ICPR)*.

Guo, Y., Zhao, G., and Pietikinen, M. (2012). Discriminative features for texture description. *Pattern Recognition*, 45(10):3834 – 3843.

Guo, Z., Zhang, L., and Zhang, D. (2010). A completed modeling of local binary pattern operator for texture classification. *IEEE Transactions on Image Processing*, 19(6):1657–1663.

Guo, Z., Zhang, L., and Zhang, D. (2010). Rotation invariant texture classification using lbp variance (lbpv)

with global matching. *Pattern Recognition*, 43(3):706 – 719.

Jebali, H., Richard, N., Chatoux, H., and Naouai, M. (2018). Relocated colour contrast occurrence matrix and adapted similarity measure for colour texture retrieval. In *Advanced Concepts for Intelligent Vision Systems*, pages 609–619, Cham. Springer International Publishing.

Jesús, A. (2014). Riemannian l (p) averaging on lie group of nonzero quaternions. *Advances in Applied Clifford Algebras*, 24.

Khadiri, I. E., Chahi, A., Merabet, Y. E., Ruichek, Y., and Touahni, R. (2018). Local directional ternary pattern: A new texture descriptor for texture classification. *Computer Vision and Image Understanding*, 169:14 – 27.

Kullback, S. and Leibler, R. (1951). On information and sufficiency. *Ann. Math. Statist*, 22(1):79–86.

Maliani, A. D. E., Hassouni, M. E., Berthoumieu, Y., and Aboutajdine, D. (2014). Color texture classification method based on a statistical multi-model and geodesic distance. *Journal of Visual Communication and Image Representation, Elsevier*.

Manisha, V. and Balasubramanian, R. (2017). Local neighborhood difference pattern: A new feature descriptor for natural and texture image retrieval. *Multimedia Tools and Applications*, pages 1–25.

Martinez, R., Richard, N., and Fernandez, C. (2015). Alternative to colour feature classification using colour contrast ocurrence matrix. *Proc. SPIE 9534, Twelfth International Conference on Quality Control by Artificial Vision*.

Mehta, R. and Egiazarian, K. (2016). Dominant rotated local binary patterns (drlbp) for texture classification. *Pattern Recognition Letters*, 71:16 – 22.

Merabet, Y. E. and Ruichek, Y. (2018). Local concave-and-convex micro-structure patterns for texture classification. *Pattern Recognition*, 76:303 – 322.

Merabet, Y. E., Ruichek, Y., and Idrissi, A. E. (2019). Attractive-and-repulsive center-symmetric local binary patterns for texture classification. *Engineering Applications of Artificial Intelligence*, 78:158 – 172.

Minh-Tan, P., Grgoire, M., and Lionel, B. (2017). Color texture image retrieval based on local extrema features and riemannian distance. *Journal of Imaging*, 3(4).

Neiva, M. B., Vacavant, A., and Bruno, O. M. (2018). Improving texture extraction and classification using smoothed morphological operators. *Digital Signal Processing*, 83:24 – 34.

Ojala, T., Pietikainen, M., and Maenpaa, T. (2002). Multiresolution gray-scale and rotation invariant texture classification with local binary patterns. *IEEE Transactions on Pattern Analysis and Machine Intelligence*, 24(7):971–987.

Oliveira, M. W. D. S., da Silva, N. R., Manzanera, A., and Bruno, O. M. (2015). Feature extraction on local jet space for texture classification. *Physica A: Statistical Mechanics and its Applications*, 439:160 – 170.

Penatti, O. A., Valle, E., and da S. Torres, R. (2012). Comparative study of global color and texture descriptors for web image retrieval. *Journal of Visual Communication and Image Representation*, 23(2):359 – 380.

Richard, N., Martinez, R., and Fernandez, C. (2016). Colour local pattern: a texture feature for colour images. *Journal of the International Colour Association*, 16:56–68.

Rowan, H. W. (London 1866). *Elements of Quaternions*. Longmans Green.

Sangwine, S. J. (1996). Fourier transforms of colour images using quaternion or hypercomplex, numbers. *Electronics Letters*, 32(21):1979–1980.

Timo, A., Abdenour, H., and Matti, P. (2004). Face recognition with local binary patterns. In Pajdla, T. and Matas, J., editors, *Computer Vision - ECCV 2004*, pages 469–481, Berlin, Heidelberg. Springer Berlin Heidelberg.

Xiaoyan, S., Shao-Hui, C., Jiang, L., and Frederic, M. (2009). Automatic diagnosis for prostate cancer using run-length matrix method. *Medical Imaging. Proceeding of SPIE*, 7260.